

Steady-state and Transient Temperature Distributions of Fuel and Coolant in Radial and Axial Directions in a Cylindrical Nuclear Fuel Element

M.A. Mehrabian¹

Steady-state and transient temperature distributions throughout a nuclear fuel element composed of fuel, gap and clad regions as well as the mean coolant temperature are predicted using a finite difference conduction-convection numerical analysis. The implicit Crank-Nicolson scheme is used to predict temperature in the fuel pin nodes and the mean coolant temperature in each axial section. These temperatures are then used to solve the explicit governing equation for the coolant and give the outlet temperature from each axial section. The numerical analysis is based on energy equation for a node, to make sure that energy is always conserved in a strict sense, especially at the boundaries of four different regions (fuel, gap, clad, coolant) when the adjacent nodes belong to the non-homogeneous regions.

Keywords: Heat conduction equation – Analytical, numerical approach – Accuracy, stability and truncation error.

1. Introduction

In nuclear reactors, the temperature field in fuel elements changes as a result of heat generated from the fission interactions inside the fuel elements. The temperature distribution in nuclear fuel elements in steady-state and transient regimes provides important information regarding the cooling system which should be designed in a way that absorbs heat from the reactor core while safety considerations are taken into account [1]. In this paper, the analytical approach to solve the heat conduction equation in a homogeneous cylindrical fuel element is introduced, followed by the finite difference numerical method based on energy balance equation for a node.

The heat conduction equation in a nuclear fuel element is [2]:

$$\frac{\partial T}{\partial t} = \alpha (\nabla^2 T + \frac{q}{k}) \quad \text{.....(1)}$$

in which, q is the rate of heat generation per unit volume, k thermal conductivity, α thermal diffusivity and $T(r, t)$ temperature function in the fuel element. The fuel element is assumed to have cylindrical shape having radius a with negligible temperature changes in axial direction. Therefore, Eq. 1 is reduced to:

$$\frac{\partial T}{\partial t} = \alpha \left(\frac{\partial^2 T}{\partial r^2} + \frac{1}{r} \frac{\partial T}{\partial r} + \frac{\partial^2 T}{\partial \theta^2} + \frac{q}{k} \right) \quad \text{.....(2)}$$

Considering the axial symmetry of the cylindrical fuel element, Eq. 2 becomes:

$$\frac{\partial T}{\partial t} = \alpha \left(\frac{\partial^2 T}{\partial r^2} + \frac{1}{r} \frac{\partial T}{\partial r} + \frac{q}{k} \right) \quad \text{.....(3)}$$

We may assume that in the time interval $t \in (\infty - 0)$, temperature variations with respect to time are

¹ Department of Mechanical Engineering, Shahid Bahonar University of Kerman, P.O. Box 76169-133, Kerman, Iran.
E.mail: ma_mehrabian@yahoo.com

negligible; where time $t=0$ corresponds to the shut down period. Thus, Eq. 3 becomes:

$$\frac{\partial^2 T}{\partial r^2} + \frac{1}{r} \frac{\partial T}{\partial r} + \frac{q}{k} = 0 \quad \text{.....(4)}$$

or,

$$\frac{\partial T}{\partial r} = -r \left(\frac{\partial^2 T}{\partial r^2} + \frac{q}{k} \right) \quad \text{.....(5)}$$

Eq. 5 indicates that when $r=0$, then $\frac{\partial T}{\partial r} \Big|_{r=0, t=0} = 0$, that is, at time $t=0$ the temperature at fuel centre is constant and may be called T_m , though,

$$T(0,0) = T_m \quad \text{.....(6)}$$

To solve Eq. 4, the following homogeneous equation is solved first,

$$\frac{\partial^2 T}{\partial r^2} + \frac{1}{r} \frac{\partial T}{\partial r} = 0 \quad \text{.....(7)}$$

The solution to the above equation is:

$$T = c_1 \ln r + c_2 \quad \text{.....(8)}$$

Applying the conditions at fuel centre, (Eq. 6), gives the values of $c_1 = 0$ and $c_2 = T_m$ which reduces Eq. 8 into:

$$T = T_m \quad \text{.....(9)}$$

The non-homogeneous version of Eq. 7, is written as follows:

$$\frac{\partial^2 T}{\partial r^2} + \frac{1}{r} \frac{\partial T}{\partial r} = -\frac{q}{k} \quad \text{.....(10)}$$

The specific solution to the above equation is:

$$T = Ar^2 + Br + C \quad \text{.....(11)}$$

Differentiating the above equation and applying into Eq. 10 gives the values of $A = -q/4k$, $B=0$, and $C=0$ which reduces the above equation into:

$$T = -\frac{qr^2}{4k} \quad \text{.....(12)}$$

Thus, a general solution to Eq. 4, when $(t \leq 0)$ would be the sum of Eqs. 9 and 12:

$$T(r,t) = T_m - \frac{qr^2}{4k} \quad (t \leq 0) \quad \text{.....(13)}$$

Theoretically, if the fuel is covered by insulation and the insulation effectively prevents heat to escape, the rate of temperature changes at the wall is zero, thus:

$$\frac{\partial T}{\partial r} \Big|_{r=a, t=t} = 0$$

Therefore, the heat conduction equation for the fuel element and its boundary and initial conditions are:

$$\frac{\partial T}{\partial t} = \alpha \left(\frac{\partial^2 T}{\partial r^2} + \frac{1}{r} \frac{\partial T}{\partial r} + \frac{q}{k} \right) \quad \text{.....(14a)}$$

$$\frac{\partial T}{\partial r} \Big|_{r=a} = 0 \quad \text{.....(14b)}$$

$$T(r,0) = T_m - \frac{qr^2}{4k} \quad \text{.....(14c)}$$

We may further assume, after the reactor is shut down $(t > 0)$, there is no heat generation $(q=0)$, thus, Eqs. 14(a), 14(b) and 14(c) become:

$$\frac{\partial T}{\partial t} = \alpha \left(\frac{\partial^2 T}{\partial r^2} + \frac{1}{r} \frac{\partial T}{\partial r} \right) \quad \text{.....(15a)}$$

$$\left. \frac{\partial T}{\partial r} \right|_{r=a} = 0 \quad \text{.....(15b)}$$

$$T(r,0) = T_m - \frac{qr^2}{4k} \quad \text{.....(15c)}$$

To separate the variables, we assume:

$$T(r,t) = f(r)g(t) \quad \text{.....(16)}$$

$$\frac{1}{\alpha} \frac{g'}{g} = -p^2 \quad \text{.....(17)}$$

$$\frac{f''}{f} + \frac{1}{r} \frac{f'}{f} = -p^2 \quad \text{.....(18)}$$

The solution to Eq. 17 is:

$$g(t) = A_1 \exp(-p^2 \alpha t) \quad \text{.....(19)}$$

The general solution to Eq. 18 is:

$$f(r) = A_2 J_0(pr) \quad \text{.....(20)}$$

in which,

$$J_0(pr) = \sum_{k=0}^{\infty} \frac{(-1)^k}{(k!)^2} \left(\frac{pr}{2}\right)^{2k} = 1 - \frac{(pr)^2}{2^2} + \frac{(pr)^4}{2^2 4^2} - \frac{(pr)^6}{2^2 4^2 6^2} + \dots \quad \text{.....(21)}$$

Substituting Eqs. 19 and 20 into Eq. 16a gives:

$$T(r,t) = A \exp(-p^2 \alpha t) J_0(pr) \quad (t > 0) \quad \text{.....(22)}$$

Differentiating Eq. 22 with respect to r gives:

$$\frac{\partial T}{\partial r} = A p \exp(-p^2 \alpha t) J_0'(pr) =$$

$$-A p \exp(-p^2 \alpha t) J_1(pr) \quad \text{.....(23)}$$

Eq. 22 satisfies the boundary condition expressed in Eq. 15b, giving:

$$J_1(pa) = 0 \quad \text{.....(24)}$$

Assuming $z_n (n \in N \cup \{0\})$ are the roots of Eq. 24, we then have:

$$pa = z_n \Rightarrow p = \frac{z_n}{a} \quad n \in N \cup \{0\} \quad \text{.....(25)}$$

Eq. 22 then becomes:

$$T_n(r,t) = A_n \exp\left(-\frac{z_n^2}{a^2} \alpha t\right) J_0\left(z_n \frac{r}{a}\right) \quad \text{.....(26)}$$

The first positive zeros of $J_1(pa)$ are as follows [4]:

$$(13.3237, 10.1735, 7.0156, 3.8317)$$

The function $T'(r,t)$ is defined as:

$$T'(r,t) = \sum_{k=1}^{\infty} T_k(r,t) \quad \text{.....(27)}$$

That means at $T > 0$, we have:

$$T'(r,t) = \sum_{k=1}^{\infty} A_k \exp\left(-\frac{z_k^2}{a^2} \alpha t\right) J_0\left(z_k \frac{r}{a}\right) \quad \text{.....(28)}$$

Comparing Eqs. 28 and 15c and considering the continuity of the temperature function at $t=0$, we have:

$$\lim_{t \rightarrow 0^+} T'(r,t) = T(r,0) \quad \text{.....(29)}$$

Therefore,

$$\sum A_k J_0\left(z_k \frac{r}{a}\right) = T_m - \frac{qr^2}{4k} \quad \text{.....(30)}$$

Differentiating Eq. 30 with respect to r gives:

$$\sum_{k=1}^{\infty} \frac{A_k z_k}{a} J_0'(z_k \frac{r}{a}) = -\frac{qr}{2k} \quad \text{.....(31)}$$

and,

$$\sum_{k=1}^{\infty} \frac{A_k z_k}{a} J_1(z_k \frac{r}{a}) = \frac{qr}{2k} \quad \text{.....(32)}$$

in which, $0 \leq r \leq a$ or $0 \leq \frac{r}{a} \leq 1$. Assuming $t = \frac{r}{a}$ and $a_k = A_k z_k$ results in:

$$\sum_{k=1}^{\infty} a_k J_1(z_k t) = \frac{qa^2 r}{2k} \quad \text{.....(33)}$$

in which z_k are the positive zeros of function $J_1(x)$. We can therefore write [5]:

$$a_k = \frac{2}{J_2(z_k)^2} \int_0^1 \frac{qa^2 t^2}{2k} J_1(z_k t) dt \quad \text{.....(34)}$$

replacing k by n and assuming $A_n = \frac{a_n}{z_n}$, Eq. 34 becomes:

$$A_n = \frac{qa^2}{kz_n^2 J_2(z_n)^2} \int_0^1 t^2 J_1(z_n t) dt \quad \text{.....(35)}$$

Applying the recurrence relation [6] into Eq. 35 and assuming $z_0 = 0$ gives:

$$A_n = \frac{qa^2 J_0(z_n)}{kz_n^2 J_2(z_n)^2} \quad (n=1,2,3,...) \quad \text{.....(36)}$$

We may define function $T(r, t)$ as follows:

$$T(r, t) = A_0 + T^1(r, t) \quad \text{.....(37)}$$

or,

$$T(r, t) = \sum_{k=0}^{\infty} A_k \exp(-\frac{z_k^2 \alpha t}{a^2}) J_0(z_k \frac{r}{a}) \quad \text{.....(38)}$$

The following results are obtained from the above equation:

$$\lim_{t \rightarrow +\infty} T(r, t) = A_0 \quad \text{.....(39)}$$

$$T(0, t) = \sum_{k=0}^{\infty} A_k \exp(-\frac{z_k^2 \alpha t}{a^2}) \quad \text{.....(40)}$$

$$T_m = T(0, 0) =$$

$$\sum_{k=1}^{\infty} A_k = A_0 + \sum_{k=1}^{\infty} A_k \quad \text{.....(41)}$$

$$A_0 = T_m - \sum_{k=1}^{\infty} A_k =$$

$$T_m + \frac{qa^2}{k} \sum_{k=1}^{\infty} \frac{J_0(z_n)}{z_n^2 J_2(z_n)} \quad \text{.....(42)}$$

It can easily be seen that $\sum_{n=1}^{\infty} A_n$ is convergent and furthermore,

$$0 < A_0 < \sum_{n=1}^{\infty} A_n < T_m$$

from Eq. 40 we have,

$$T(0, t) = \sum_{n=0}^{\infty} A_n \exp(-\frac{z_n^2 \alpha t}{a^2})$$

When $0 \leq r \leq a$, we have $J_0(z_n \frac{r}{a}) < J_0(0) = e^0 = 1$, therefore:

$$T(r,t) = \sum_{n=0}^{\infty} A_n \exp\left(-\frac{z_n^2 \alpha t}{a^2}\right)$$

$$J_0\left(z_n \frac{r}{a}\right) \leq T(r,t) \leq T_m \quad \dots\dots\dots(43)$$

It can be observed that $T(r,t)$ at the centre of fuel element ($r=0$), is a descending, while at the wall ($r=a$) is an ascending function and at each time t , we have:

$$T(a,t) \leq A_0 \leq T(0,t) \quad \dots\dots\dots(44)$$

Detailed descriptions of this subject covering key issues such as radial power depression, burnup and densification are available in [8] and [9].

2. Numerical Solution Method

A finite difference conduction-convection computer programme written in Fortran IV is designed to calculate one-dimensional steady and transient temperature distributions throughout a nuclear fuel element composed of fuel, gap and clad regions as well as the mean coolant temperature (Figure 1). Stability and speed (less computation time) are the most significant criteria for this programme. Cylindrical geometry, axial symmetry, single phase flow and radial space variation are the underlying assumptions. Furthermore, the rod and coolant channel are divided into an arbitrary number of axial divisions (Figure 2). Within each axial section, the heat generation is assumed uniform in the fuel region and heat transport in the element is considered to occur in the radial direction. The number of nodes in the fuel and the cladding may be specified arbitrarily.

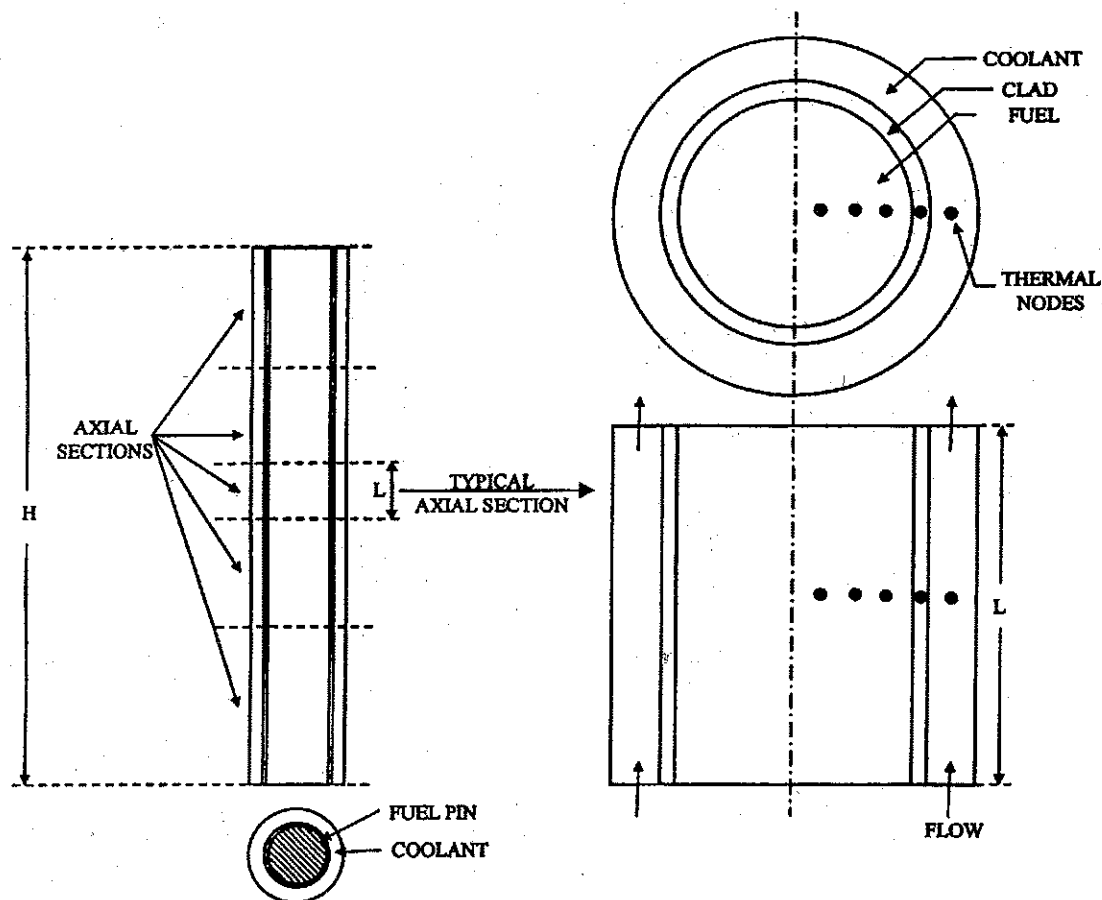


FIGURE 1: Nodalisation of the Reactor Geometry for Thermal Analysis

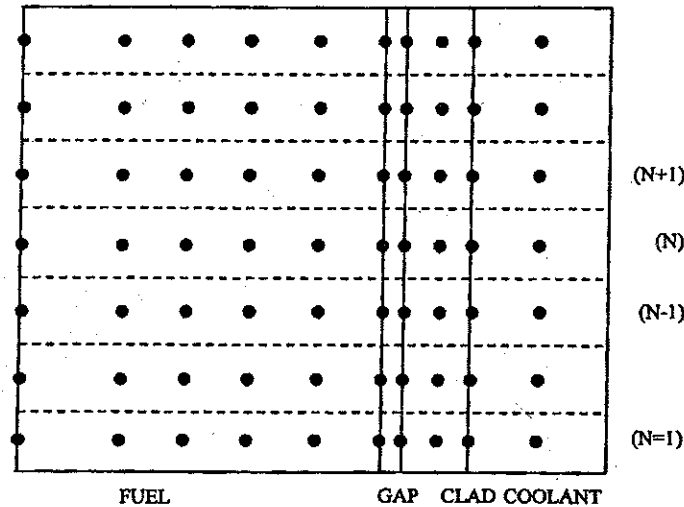


FIGURE 2: Illustration of Axial Divisions

The programme requires numerical input data that specify the initial conditions and the heat generation in the fuel, mass flow rate of the coolant and the inlet temperature of the coolant as functions of time. In addition, the user may specify constant values of thermal conductivity and heat transfer coefficients or provide tables, which the programme uses to calculate variable properties.

The programme is based on the Crank-Nicolson scheme and considers the nodal points in the middle of radial divisions (Figure 3). Thermal properties vary from one radial section to another and they are specified in a backward difference manner as well as geometry factors, i.e., km for example indicates conductivity between nodes m and $(m-1)$.

The programme consists of six subroutines and a main programme. All computational work is done in

the subroutines. The main programme serves to call them in the proper sequence and print out results.

Subroutine 1 reads most of the input data, initialises most variables and then prints out a summary of the input. If a steady state initial condition is specified, the main programme then calls Subroutine 2, which calculates a steady state temperature distribution based on input heat generation, coolant inlet temperature and constant thermal properties. At this point, all initial conditions for the calculation are known.

The first step in calculating temperatures for the first time increment is to determine the outlet coolant temperature of each axial division. This is done explicitly in Subroutine 3. The calculational procedure is based on the method of Bender [7]. With the inlet and outlet temperatures of each axial division known, the mean coolant temperature and the nodal temperatures in the fuel pin are combined in an implicit (Crank-Nicolson) manner to solve for their values at the next time step. Subroutine 4 performs this calculation using forward elimination and backward substitution (Thomas algorithm) to solve the tridiagonal matrix setup for each axial section. Subroutine 5 takes care of the pellet thermal expansion and gap closure behaviour.

The main programme now writes out the calculated temperature values, if required to do so, sets the values of the previous step equal to the present ones, then begins the calculations for the next time increment.

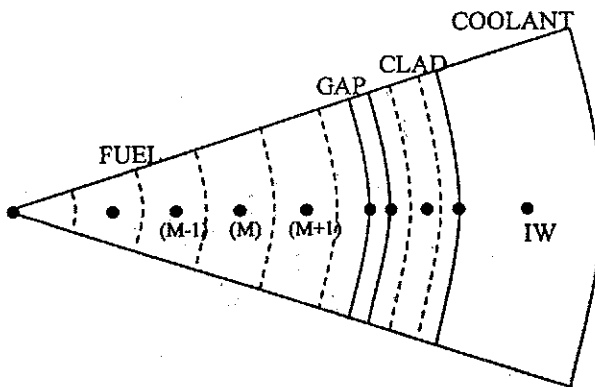


FIGURE 3: Nodal Structure in Fuel Pin with Nomenclature used in Computer Programme

3. Energy Equation for the Coolant

The governing equation for the coolant temperature is:

$$\rho CA \frac{\partial T_w(t, z)}{\partial t} + \rho CAV \frac{\partial T_w(t, z)}{\partial z} = 2\pi r q''$$

.....(45)

This is a lumped parameter formulation and considers only the axial and temporal variation of T_w (the mean coolant temperature, independent of radius). It is solved by assuming a steady state initial condition based on initial heat flux from the fuel (q_o'') and initial flow velocity (V_o). This initial condition is stated as:

$$T_w(0, z) = T_w(0, 0) + \frac{2\pi r q_o''}{\rho CA V_o} z = T_w(0, 0) + b \frac{q_o''}{V_o} z$$

.....(46)

where,

$$b = \frac{2\pi r}{\rho CA}$$

The boundary condition for the solution is a step change in coolant inlet temperature,

$$T_w(t, 0) = T_m$$

.....(47)

Hence the initial and boundary conditions incorporate step changes in heat flux, inlet temperature and flow velocity. The solution to Eq. 45 under the assumed conditions, by Laplace transform method, is:

$$T_w(0, z) = T_w(0, z) + bV \left(\frac{q''}{V} - \frac{q_o''}{V_o} \right) t \quad (z < Vt)$$

.....(48a)

$$T_w(0, z) = T_w(t, 0) + b \frac{q''}{V} z \quad (z > Vt)$$

.....(48b)

Where Vt is the distance the perturbation has propagated up the coolant channel from $z=0$ and $T=0$. If L is an axial step size at the outlet of an axial section ($z=L$), Eqs. 48 becomes:

$$T_w(t, L) = T_w(0, L) + bV \left(\frac{q''}{V} - \frac{q_o''}{V_o} \right) t \quad (L < Vt)$$

.....(49a)

$$T_w(t, L) = T_w(t, 0) + b \frac{q''}{V} L \quad (L > Vt)$$

.....(49b)

where, according to Eq. 46,

$$T_w(0, L) = T_w(0, 0) + bL \frac{q_o''}{V_o}$$

or:

$$q_o'' = \frac{V_o}{bL} [T_w(0, L) - T_w(0, 0)]$$

.....(50)

In addition, we know:

$$q'' = h(T - T_w)$$

.....(51)

Combining Eqs. 50 and 51 with Eqs. 49 and defining:

$$T_L(t) = T_w(t, L)$$

$$T_L^j = T_L(t^j)$$

$$T_L^{j+1} = T_L(t^{j+1})$$

$$\Delta\tau = t^{j+1} - t^j$$

$$w_c = \frac{2\pi rh}{\rho CA} = bh$$

$$\lambda = L/V$$

a finite difference form for Eqs. 49 is obtained:

$$T_L^{j+1} = T_L^j - (T_L^j - T_w^j) \frac{\Delta\tau}{\lambda} +$$

$$w_c(T^j - T_w^j)\Delta\tau \quad (\Delta\tau > \lambda) \quad \dots\dots(52a)$$

$$T_L^{j+1} = T_L^j + w_c(T^j - T_w^j)\Delta\tau \quad (\Delta\tau < \lambda) \quad \dots\dots(52b)$$

Bender [7] found that in actual practice, due to the likelihood of non-linear temperature profiles in an axial section, a better finite difference formulation for Eqs. 49, which includes a linear variation of inlet temperature, would be:

$$T_L^{j+1} = T_L^j - (T_L^{j+1} - T_w^j) \frac{2\Delta\tau}{\lambda} + w_c(T^j - T_w^j)\Delta\tau \quad (\Delta\tau > \lambda) \quad \dots\dots(53a)$$

$$T_L^{j+1} = T_L^j + \frac{T_w^{j+1} - T_w^j}{\Delta\tau}(\Delta\tau - \lambda) + w_c(T^j - T_w^j)\Delta\tau \quad (\Delta\tau < \lambda) \quad \dots\dots(53b)$$

Eqs. 52 are the expressions used in the computer programme to evaluate the outlet temperatures from each axial section. To solve these equations, we need to know T^j (temperature in the fuel element nodes) and T_w^j (mean coolant temperature in each axial section) which are evaluated from an implicitly formulated energy balance on each node.

4. Energy Equation for a Node

The heat conduction equation is the basis for any finite difference formulation, i.e., partial derivatives of the differential equation are approximated by difference expressions. In this programme, when four different regions (fuel, gap, clad and coolant) are present, it seems advantageous to start with the energy balance equation, to make sure that energy is always conserved in a strict sense especially at the boundaries when the adjacent nodes belong to the non-homogeneous regions. Looking at **Figure 4**, the energy balance on a node can simply be expressed as:

$$Q_{in} + Q_{gen} = Q_{out} + Q_{store} \quad \dots\dots(54)$$

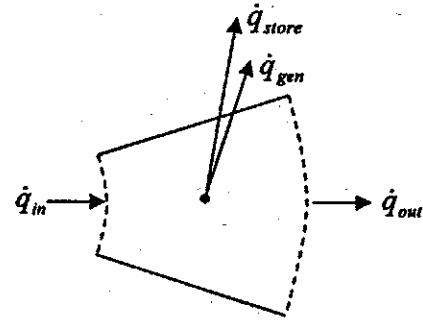


FIGURE 4: Energy Balance on a Node

Each term is expressed in terms of temperature variations at adjacent points, the Crank-Nicolson method will lead to:

$$Q_{in} = -k_{m,n}A_m(\Delta z) \frac{T_{m,n}^{j+1} - T_{m-1,n}^{j+1} + T_{m,n}^j - T_{m-1,n}^j}{2\Delta r_m}$$

$$Q_{gen} = B_m q_n(\Delta z)$$

$$Q_{out} = -k_{m+1,n}A_{m+1}(\Delta z) \frac{T_{m+1,n}^{j+1} - T_{m,n}^{j+1} + T_{m+1,n}^j - T_{m,n}^j}{2\Delta r_{m+1}}$$

$$Q_{store} = \rho CB_m(\Delta z) \frac{T_{m,n}^{j+1} - T_{m,n}^j}{\Delta\tau}$$

where,

$$A_m = 2\pi(RA)_m$$

$$(RA)_m = \frac{r_m + r_{m+1}}{2}$$

$$B_m = \pi[(RA)_{m+1}^2 - (RA)_m^2]$$

Substituting these results into Eq. 54 yields:

$$\begin{aligned} & -\frac{A_m k_{m,n}}{2\Delta r_m} T_{m-1,n}^{j+1} + \left(\frac{\rho C B_m}{\Delta \tau} \right. \\ & \left. + \frac{A_m k_{m,n}}{2\Delta r_m} + \frac{A_{m+1} k_{m+1,n}}{2\Delta r_{m+1}} \right) \\ & T_{m,n}^{j+1} - \frac{A_{m+1} k_{m+1,n}}{2\Delta r_{m+1}} T_{m+1,n}^{j+1} = \\ & q_n B_m + \frac{A_m k_{m,n}}{2\Delta r_m} T_{m-1,n}^j + \\ & \left(\frac{\rho C B_m}{\Delta \tau} - \frac{A_m k_{m,n}}{2\Delta r_m} - \frac{A_{m+1} k_{m+1,n}}{2\Delta r_{m+1}} \right) T_{m,n}^j + \\ & \frac{A_{m+1} k_{m+1,n}}{2\Delta r_{m+1}} T_{m+1,n}^j \end{aligned} \quad \text{.....(55)}$$

This equation remains unchanged in form throughout the fuel, gap and clad regions. At convective boundaries (fuel-gap), gap-clad), the heat transfer conductance term $A_m k_{m,n} / 2\Delta r_m$ is replaced by (hA_m) , where h is the convective heat transfer coefficient.

It should be noticed that there can be as many nodal points in the clad region as desired and Eq. 55 supplies one equation for each point. The coolant temperature has to satisfy the coolant energy equation which is achieved by an energy balance on the coolant node,

$$\begin{aligned} T_{w,n}^{j+1} &= T_{w,n}^j + \frac{w_c(\Delta \tau)}{2} [T_{ICO,n}^{j+1} + \\ & T_{ICO,n}^j - T_{w,n}^{j+1} - T_{w,n}^j] \\ & - \frac{\Delta \tau}{2\lambda} (T_{L,n}^j - T_{L,n-1}^j) - \frac{\Delta \tau}{\lambda} (T_{w,n}^{j+1} - T_{w,n-1}^j) \end{aligned} \quad \text{.....(56)}$$

Rearranging,

$$\begin{aligned} & -\frac{w_c(\Delta \tau)}{2} T_{ICO}^{j+1} + \left[1 + \frac{w_c(\Delta \tau)}{2} + \frac{\Delta \tau}{\lambda} \right] T_{w,n}^{j+1} = \\ & T_{w,n}^j + \frac{w_c(\Delta \tau)}{2} [T_{ICO,n}^j - T_{w,n}^j] \\ & - \frac{\Delta \tau}{2\lambda} (T_{L,n}^j - T_{L,n-1}^j) + \frac{\Delta \tau}{\lambda} T_{L,n-1}^{j+1} \end{aligned} \quad \text{.....(57)}$$

Eq. 55 together with Eq. 57 form a tridiagonal matrix, because any equation contains three unknowns (based on knowing temperatures at time j). The system of simultaneous linear algebraic equations is solved using Thomas algorithm to give the temperatures of the system at the advanced time step.

5. Stability Analysis

The time increment ($\Delta \tau$) and the mesh size in axial direction (Δz) should be selected in a way that the following stability criterion is met:

$$SC = \Delta \tau V / \Delta z \leq 1 \quad \text{.....(58)}$$

That means, the time increment ($\Delta \tau$) must be equal to or less than the transient time of the flow through one axial section ($\Delta z / V$).

In addition to Eq. 58, the general equipment for an implicit finite difference formulation [5] should be satisfied:

$$\frac{\alpha \Delta \tau}{r \Delta r} \leq \frac{1}{2} \quad \dots\dots(59)$$

6. Results

A sample problem for the case of a typical UO_2 fuelled fuel pin, involving a step change in coolant inlet temperature from the steady state value of 134.4°C to 287.8°C is studied. There are 12 vertical divisions and nine nodal locations in the fuel pin (six in the fuel and three in the clad). The gap heat transfer coefficient is given a constant value of $66.1 \text{ kW/m}^2\text{K}$, but conductivities and coolant heat transfer coefficients are variable and tables of their values are read in. The heat generation is constant ($3.38 \times 10^8 \text{ W/m}^3$) all over the rod and the mass flow rate is also constant (0.425 kg/s).

For the steady-state calculations, a UO_2 thermal conductivity of 40.3 W/mK is used, as is 262 W/mK for the clad and $661 \text{ kW/m}^2\text{K}$ for the coolant heat transfer coefficient.

The height of the core is 3.6576 m , making each division 0.3048 m . The fuel radius is 4.66 mm , followed by a gap of 0.1646 mm . The clad outer radius is 5.36 mm and the coolant channel is 8.3 mm in radius.

Table 1 indicates the programme's predictions for fuel centre line, $T(1,N,1)$, fuel outer surface, $T(1F,N,1)$, and for the purpose of shortening, only one selected nodal point in the fuel, $T(3,N,1)$, as well as clad inner surface, $T(1CI,N,1)$, clad outer surface, $T(1CO,N,1)$, and the coolant, $T_w(N,1)$, temperatures in steady state condition at 12 different axial divisions.

Table 2 indicates the programme's predictions for fuel center line, $T(1,N,8)$, fuel outer surface, $T(1F,N,8)$, and for the purpose of shortening, only one selected nodal point in the fuel, $T(3,N,8)$, as well as, clad inner surface, $T(1CI,N,8)$, clad outer surface, $T(1CO,N,8)$, and the coolant, $T_w(N,8)$, temperatures after eight time increments at 12 different axial divisions.

7. Discussion

A finite difference conduction-convection computer programme is developed to predict one-dimensional steady and transient temperature profiles throughout a nuclear fuel element composed of fuel, gap and clad regions as well as the mean coolant temperature. The programme takes advantage of the implicit Crank-

Nicolson scheme and energy balance approach. Thermal properties are temperature dependent and nodal points are in the middle of radial divisions. The thickness of radial divisions is not uniform and the number of nodes in clad is unlimited. The stability requirements are defined by Eqs. 58 and 59. The CPU for standard priority to run the programme for steady state and eight time increments is about 8 seconds. The order of error is:

$$O(\Delta t^2) + O(\Delta x^2) + \text{error in } q$$

The effect of time increment on coolant outlet temperature is studied using coolant inlet temperature as the transient. Coolant inlet temperature is subjected to a step change and the programme is run with two different time increments. **Figure 5** shows when the criteria of Eq. 58 is violated, $\Delta \tau V / \Delta z = 4$, the programme does not properly handle the propagation of the perturbation up the channel, and the results become inaccurate.

The effect of time increment on the maximum fuel and clad temperatures is studied when coolant mass flow rate and fuel heat generation are the transients. LOCA-like coolant mass flow rate (**Figure 6**) and fuel heat generation (**Figure 7**) are input variables, system nodal temperature variations are presented in **Figure 8**.

The effect of time increment on coolant outlet temperature is studied when coolant inlet temperature is the transient. Coolant inlet temperature is subjected to a linear ramp change rather than a step change which was described before. **Figure 9** shows the coolant outlet temperature at time 0.2 s when Eq. 58 is violated. The same analysis is done at time 0.4 s in **Figure 10**.

8. Conclusions

The transient thermal response of a reactor fuel rod and coolant channel to reactivity and flow perturbations are studied numerically. Large and rapid transients are handled in the minimum computation time, while stability and speed are greatly appreciated.

The gap heat transfer coefficient is either constant or supplied by the programme. The programme encompasses geometries ranging from an open gap with partial fuel-to-cladding contact to a closed gap with solid-to-solid contact.

TABLE 1: Computed Results evaluated by the Programme in Steady State Condition

| T(1,N,0) | T(3,N,0) | T(ICI,N,0) | T(ICO,N,0) | T _w (N,0) | T(1,N,0) | N | |
|----------|----------|------------|------------|----------------------|----------|----|---|
| 835.4 | 623 | 304.5 | 165.6 | 148.5 | 136.4 | 1 | 0 |
| 838.2 | 625.9 | 307.3 | 168.4 | 151.3 | 139.2 | 2 | 0 |
| 841 | 628.7 | 310.2 | 171.3 | 154.1 | 142.1 | 3 | 0 |
| 843.9 | 631.5 | 313 | 174.1 | 157 | 144.9 | 4 | 0 |
| 846.7 | 634.3 | 315.8 | 176.9 | 159.8 | 147.7 | 5 | 0 |
| 849.5 | 637.2 | 318.6 | 179.8 | 162.6 | 150.6 | 6 | 0 |
| 852.4 | 640 | 321.5 | 182.6 | 165.5 | 153.4 | 7 | 0 |
| 855.2 | 642.8 | 324.3 | 185.4 | 168.3 | 156.2 | 8 | 0 |
| 858 | 645.7 | 327.1 | 188.2 | 171.1 | 159 | 9 | 0 |
| 860.8 | 648.5 | 330 | 191.1 | 173.9 | 161.9 | 10 | 0 |
| 863.7 | 651.3 | 332.8 | 193.9 | 176.8 | 164.7 | 11 | 0 |
| 866.5 | 654.1 | 335.6 | 196.7 | 179.6 | 167.5 | 12 | 0 |

TABLE 2: Computed Results evaluated by the Programme after Eight Time Increments

| T(1,N,8) | T(3,N,8) | T(ICI,N,8) | T(ICO,N,8) | T _w (N,8) | T(1,N,8) | N | |
|----------|----------|------------|------------|----------------------|----------|----|--------|
| 838 | 631.2 | 367.6 | 295.8 | 289.5 | 288.2 | 1 | 0.2016 |
| 840.8 | 633.9 | 354.2 | 273.3 | 276.5 | 284.2 | 2 | 0.2016 |
| 843.7 | 636.7 | 342.9 | 231.3 | 238.2 | 252.7 | 3 | 0.2016 |
| 846.5 | 639.6 | 338.6 | 198.4 | 191.2 | 197.2 | 4 | 0.2016 |
| 849.4 | 642.5 | 339.4 | 187.7 | 166.8 | 161.6 | 5 | 0.2016 |
| 852.2 | 654.3 | 341.8 | 187.8 | 162.6 | 152.9 | 6 | 0.2016 |
| 855.1 | 648.8 | 344.4 | 190.3 | 165 | 154.1 | 7 | 0.2016 |
| 857.9 | 651.6 | 347.1 | 193 | 167.2 | 156.8 | 8 | 0.2016 |
| 860.8 | 654 | 349.7 | 195.8 | 170 | 159.6 | 9 | 0.2016 |
| 863.6 | 656.8 | 352.4 | 198.5 | 172.9 | 162.4 | 10 | 0.2016 |
| 866.5 | 659.7 | 355 | 201.3 | 175.7 | 165.3 | 11 | 0.2016 |
| 869.3 | 662.6 | 357.7 | 204 | 178.5 | 168.1 | 12 | 0.2016 |

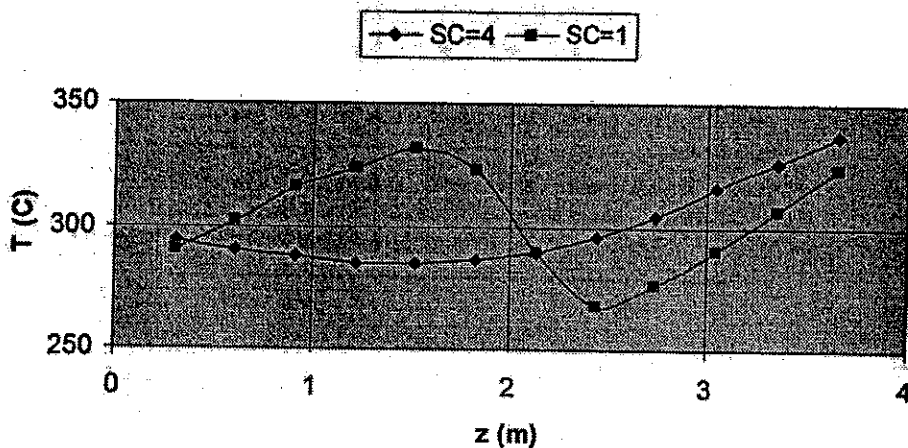


FIGURE 5: Effect of Time Increment on Coolant Outlet Temperature when Coolant Inlet Temperature is subjected to a Step Change

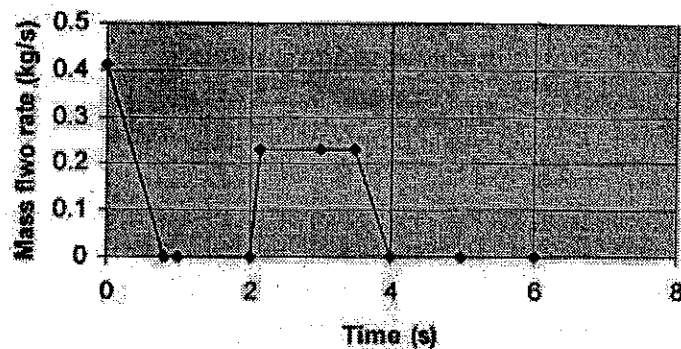


FIGURE 6: Coolant Mass Flow Rate as a Function of Time (Input Variable)

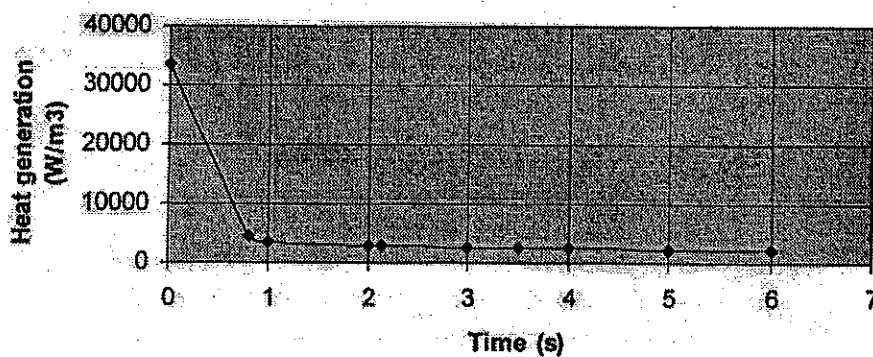


FIGURE 7: Fuel Heat Generation as a Function of Time (Input Variable)

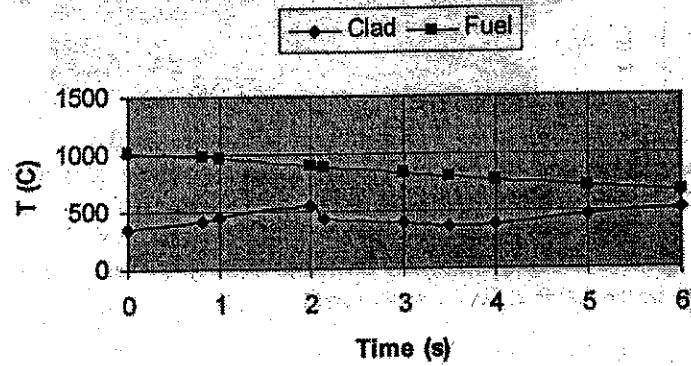


FIGURE 8: Maximum Fuel and Clad Temperatures for Rapid Variations in Mass Flow Rate and Heat Generation

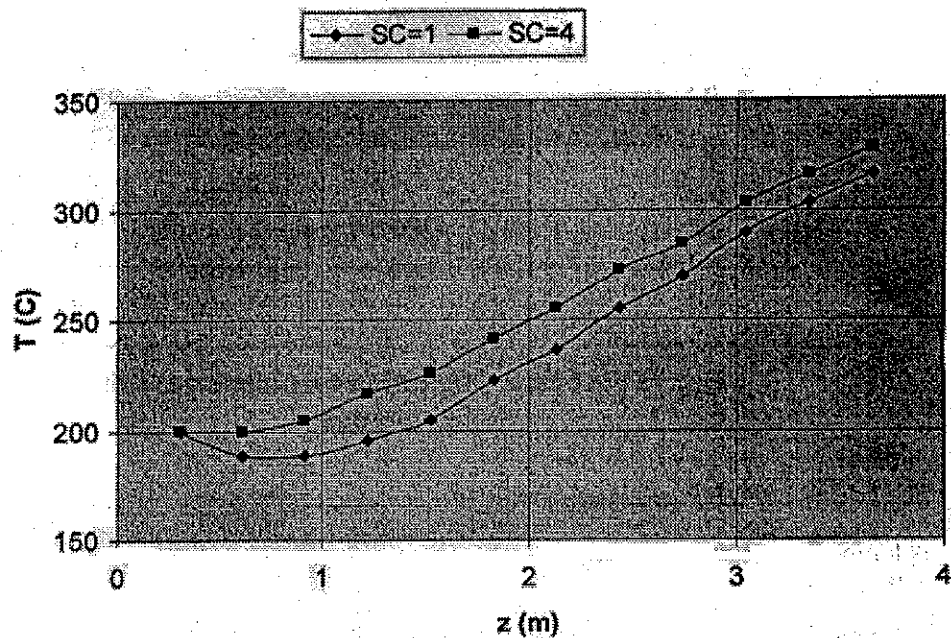


FIGURE 9: Effect of Time Increment on Coolant Outlet Temperature when Coolant Inlet Temperature is subjected to a Ramp Change (0.2 s)

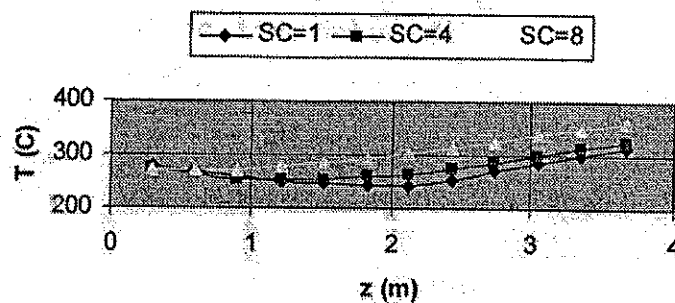


FIGURE 10: Maximum Fuel and Clad Temperatures for Rapid Variations in Mass Flow Rate and Heat Generation

The radial temperature distributions of the system are calculated in a given time increment, in two distinct steps. First, the outlet coolant temperatures (mean, independent of radius) for each axial section are calculated using a fully explicit method. Then, the radial node temperatures are computed by an implicit formulation using the previous results as input.

The coolant outlet temperature is sensitive to the variations of the coolant inlet temperature with respect to time. The maximum fuel and clad temperatures are also sensitive to the variations of mass flow rate and heat generation with respect to time.

Nomenclature

| | |
|--------------|---|
| A | Coolant flow area |
| B | Cross section area |
| A | Fuel radius |
| C | Coolant specific heat |
| H | Heat transfer coefficient |
| K | Fuel thermal conductivity |
| L | Axial division height |
| Q | Rate of heat generation |
| R | Clad inner radius |
| q'' | Heat flux from the fuel |
| q_o'' | Initial heat flux from the fuel |
| Q | Rate of heat generation per unit volume |
| RA | Average radius |
| SC | Stability criterion |
| t | Dimensionless radial distance (r/a) |
| T_m | Initial temperature at fuel center |
| T_w | Mean coolant temperature |
| T_{ICI} | Inside clad temperature |
| T_{ICO} | Outside clad temperature |
| T_{in} | Intlet coolant temperature |
| T_{IF} | Outside fuel temperature |
| T_L | Outlet coolant temperature |
| V | Coolant flow velocity |
| V_o | Initial flow velocity |
| α | Thermal diffusivity |
| λ | Time needed for coolant to move one axial section (L/V) |
| $\Delta\tau$ | Time increment |
| ρ | Coolant density |

References

- [1] El-Wakil, M.M. (1971). *Nuclear Heat Transport*, International Textbook.
- [2] Arpaci, V.S. (1966). *Conduction Heat Transfer*, Addison-Wesley.
- [3] Simmons, G.F. (1972). *Differential Equations with Applications and Historical Notes*, McGraw-Hill.
- [4] Rudin, W. (1976). *Principles of Mathematical Analysis*, 3rd edition, McGraw-Hill.
- [5] Clark, M. and Hansen, K.F. (1964). *Numerical Methods of Reactor Analysis*, Academic Press.
- [6] Hildebrand, F.B. (1952). *Methods of Applied Mathematics*, Prentice-Hall.
- [7] Bender, D. (1969). *An Explicit Unlimited Stability Approach to the Transient Conduction-Convection Equations*, Proceedings of ANS Conf. on Effective Use of Computers in the Nuclear Industry, Knoxville, Tenn., April, 1969.
- [8] Olander, (1976). *Fundamental Aspects of Nuclear Reactor Fuel Elements*. University of California, Chapter 10: Fuel element thermal performance.
- [9] CEA, (1999). *The Nuclear Fuel of Pressurized Water Reactors and Fast Reactors*, Intercept Ltd, Appendix A: Basic fuel element calculations. ■